Biogeosciences Discuss., https://doi.org/10.5194/bg-2018-511
Manuscript under review for journal Biogeosciences
Discussion started: 3 January 2019


Biogeosciences Discussions Open Access EGU

# Nutrient distribution and nitrogen and oxygen isotopic composition of nitrate in water masses of the subtropical South Indian Ocean

Natalie C. Harms[1], Niko Lahajnar[1], Birgit Gaye[1], Tim Rixen[1,2], Kirstin Dähnke[3], Markus Ankele[3], Ulrich Schwarz-Schampera[4] and Kay-Christian Emeis[1,3]

[1]Institute of Geology, Universität Hamburg, Hamburg, 20146, Germany.
[2]Leibniz-Centre for Tropical Marine Research, Bremen, 28359, Germany.
[3]Helmholtz-Zentrum Geesthacht (HZG), Institute for Coastal Research, Geesthacht, 21502, Germany.
[4]Federal Institute for Geosciences and Natural Resources (BGR), Hannover, 30655, Germany.

*Correspondence to*: Natalie C. Harms (natalie.harms@uni-hamburg.de)

**Abstract.** Vast subtropical gyres are important areas for the exchange of carbon between atmosphere and ocean in spite of low nutrient concentrations, and supposedly for the influx of reactive nitrogen to the ocean by dinitrogen fixation. To identify sources and transformation processes in the nitrogen cycle of the southern Indian Ocean subtropical gyre, we investigated concentrations of water column nutrients and stable isotope composition of nitrate of samples from two expeditions in 2016 (MSM 59) and 2017 (SO 259) in the subtropical gyre between ~30°S and the equator. Low nitrate and phosphate concentrations mark the thick mixed layer of the oligotrophic gyre with values of <5.9 µM $NO_3^-$ and <0.5 µM $PO_4^{3-}$ (<310 m; σ<26.4 kg/m³). Increased nutrient concentrations towards the equator represent the northern end of the gyre, characterized by typical strong horizontal gradients of the outcropping nutriclines. Measurements of stable isotopes of nitrate ($\delta^{15}N$ and $\delta^{18}O$) indicate isotopic maxima of $\delta^{15}N$ (>7 ‰) and $\delta^{18}O$ (>4 ‰) centred at 400−500 m, representing the preformed nitrate exported from the Southern Ocean with mode water and induced by partial N-assimilation there. Additionally, a residue of nitrate affected by denitrification in the Arabian Sea is imported into the sub-thermocline of the gyre, indicated by a strong N deficit (N*<−1 µM) within the northern study area, accompanied by elevated isotopic ratios of nitrate ($\delta^{15}N$>7 ‰; $\delta^{18}O$>3 ‰). The subtropical South Indian Ocean is thus supplied by nitrate from lateral influx of water masses that have similar isotopic character, but antagonistic origin (preformed versus regenerated). A significant contribution of $N_2$-fixation within the Indian Ocean subtropical gyre (17° S−25° S) is promoted by low nitrate to phosphate ratios in the surface layer, where approximately one-third of the nitrate in the upper ocean is derived by newly fixed N.

## 1 Introduction

The South Indian Ocean is dominated by a subtropical anticyclonic gyre (Gruber and Sarmiento, 2006; Williams and Follows, 2003), one of the major five subtropical gyres in the world's ocean. In contrast to those of the Atlantic and Pacific Oceans, where subtropical gyres occur north and south of the equator, the Indian Ocean developed only one subtropical gyre south of the equator. In comparison to the other subtropical gyres, the "Indian Ocean Subtropical Gyre" (IOSG) has been sparsely

investigated. Between 10−20° S, the South Equatorial Current marks the northern limb of the IOSG (SEC; Duing, 1970; Pickard and Emery, 1982; Woodberry et al., 1989) and separates the subtropical gyre of the South Indian Ocean from the southern equatorial Indian Ocean. In the centre of the subtropical gyre, Ekman transport leads to an intensive downwelling (Williams and Follows, 1998), which results in a deepening of thermo-, pycno- and nutriclines. These layers shoal towards the fringe of the IOSG causing steep horizontal gradients (McClain et al., 2004).

Due to the intense downwelling and the resulting deepening of nutriclines, subtropical gyres form extensive oligotrophic regions, which occupy ~40 % of the Earth's surface (McClain et al., 2004). Since the biological productivity within these oligotrophic regions is relatively low and they are often referred to as "oceanic deserts" (Clark et al., 2008). However, due to their immense size they contribute significantly to atmosphere-ocean carbon fluxes (McClain et al., 2004). Future global warming is assumed to strengthen stratification in low-latitude oceans and to expand the low productive subtropical gyres, accompanied by a decrease of the net primary production (Behrenfeld et al., 2006). This might have crucial impact on the marine nitrogen cycle. Therefore, nitrate and phosphate concentrations as well as the isotopic signature of nitrate are important indicators to study the marine nitrogen cycles (Deutsch et al., 2001; Deutsch et al., 2007; Gruber and Sarmiento, 1997; Lehmann et al., 2005; Sigman et al., 2005). The dominant source and sink of fixed, reactive nitrogen in the ocean are diazotrophic $N_2$-fixation and heterotrophic denitrification (Deutsch et al., 2001). $N_2$-fixation by diazotrophs, such as *Trichodesmium* is observed over much of the tropical and oligotrophic subtropical oceans (Karl et al., 1995; Michaels et al., 1996; Capone et al., 1997; Emerson et al., 2001). $N_2$-fixation compensating the loss of reactive nitrogen during the heterotrophic denitrification if the ocean's marine nitrogen cycle is in a steady state (Deutsch et al., 2001).

The inputs of N through $N_2$-fixation are unaccompanied by inputs of phosphorus (P), leading to a decoupling of the nitrate ($NO_3^-$) and phosphate ($PO_4^{3-}$) pool. Deviations in the $NO_3^-$ to $PO_4^{3-}$ relationship from the Redfield-stoichiometry are used to study rates of both, $N_2$-fixation and denitrification (Sigman et al., 2005). Therefore, N* is used as indicator for excesses and deficits in $NO_3^-$ relative to the global $NO_3^-/PO_4^{3-}$ ratio and is expressed by the formula

$$N^* = [NO_3^-] - 16 \times [PO_4^{3-}] + 2.9\ \mu mol\ kg^{-1}. \quad (1)$$

The concept of N* has been discussed in detail by Gruber and Sarmiento (1997) and slightly modified by Deutsch et al. (2001). The concentration of 2.9 µM was added to bring the global mean of N* to about zero (Gruber and Sarmiento, 2006).

We use stable isotopes of nitrate to distinguish between sources and sinks of fixed nitrogen and to study transfer processes in the nitrogen cycle (e.g. $N_2$-fixation, denitrification, N-assimilation). During consumption processes of nitrate, e.g. N-assimilation or denitrification, heavier isotopes ($^{15}N$ and $^{18}O$) are enriched in the residual nitrate pool, leading to elevated $\delta^{15}N$ and $\delta^{18}O$ values. The difference between the isotopic ratio of the substrate (dissolved nitrate) and the product (organic N) defines the isotopic fractionation factor ε in permil (Mariotti et al., 1981). Several culture experiments indicate a $^{15}\varepsilon:^{18}\varepsilon \sim 1$ during denitrification and N-assimilation typical for processing of preformed nitrate (Granger et al., 2004; Sigman et al., 2003; Sigman et al., 2005). In contrast, nitrification of biomass originating from $N_2$-fixation decouples N and O isotopes in nitrate

pools with a significant contribution of newly fixed N. The net balance between consumption (N-assimilation or denitrification) and production ($N_2$-fixation or nitrification) is expressed by the tracer Δ(15,18) (Sigman et al., 2005):

$$\Delta(15,18) = \left(\delta^{15}N - \delta^{15}N_{deep}\right) - {}^{15}\varepsilon_{:}^{18}\,\varepsilon \times \left(\delta^{18}O - \delta^{18}O_{deep}\right) \quad (2)$$

The $\delta^{15}N_{deep}$ and $\delta^{18}O_{deep}$ are the mean of water masses, which are taken to approximate the source of nitrate to the upper water column.

Our investigations in the South Indian Ocean are part of environmental studies in the INDEX (Indian Ocean Exploration) program for marine resource exploration by the federal Institute for Geosciences and Natural Resources (BGR), Germany, and the International Seabed Authority (ISA). The main goal of this study is to investigate the relatively unknown hydrology and the unexplored distribution of nutrients and stable isotopes of nitrate along a transect from the IOSG to the southern equatorial Indian Ocean. Therefore, we use CTD measurements and analyse seawater samples to determine nutrient concentrations and stable isotopes of nitrate ($\delta^{15}N$ and $\delta^{18}O$). First, we identify the water masses and their provenance by their unique characteristic physical properties and demonstrate their influence on the nutrient distribution and isotopic composition of water column nitrate. In a second step, we use nutrient and stable isotope data to determine nutrient sources to the IOSG and their role in the global nitrogen cycle. Our results bridge the gap between several investigations in the Arabian Sea (e.g., Brandes et al., 1998; Gaye-Haake et al., 2005; Gaye et al., 2005; Gaye et al., 2013; Ward et al., 2009) and in the Southern Ocean (e.g., Bianchi et al., 1997; DiFiore et al., 2006; DiFiore et al., 2010; Sigman et al., 1999, 2000).

## 2 Materials and Methods

### 2.1 CTD measurement and sample collection

In total, 313 seawater samples were collected at 15 CTD stations (Table 1; Fig. 1) during two expeditions with R/V *Merian* (MSM 59/2 “INDEX 2016-2”; November−December 2016) and R/V *Sonne* (SO 259 “INDEX 2017”; August−October 2017). The CTD was equipped with sensors to determine density, temperature, salinity and oxygen at overall 17 CTD stations from the surface down to the sea floor. No water samples were collected at stations 07 and 11.

The study area covers the region of the IOSG from 30°S, across the SEC at 10−20°S and towards the equator. Fourteen CTD stations (Table 1; Fig.1) are located within the IOSG from 20.36° S to 27.78° S and 67.07° E to 73.92° E. CTD 05 is located in the region of the SEC (15.08° S, 74.05° E) and at the northern end of the IOSG. The northernmost CTD stations (CTD 01, 03; 2017) at 8.81°S 75.67°E and 2.98°S 77.16°E are positioned in the southern equatorial Indian Ocean, north of the SEC. Seawater samples were collected for measurements of nutrients and stable isotopes of nitrate. Samples were filtered through a nucleopore polycarbonate filter (0.45 µm) with a metal- and silicon-free Nalgene filtration unit. The filtered water was bottled in Falcon PE tubes (45 ml) and immediately stored at −20°C during the cruise. The samples were shipped as frozen airfreight

(−20°C) to Germany. Nutrient concentrations and stable isotopes of nitrate (N and O) were determined immediately after arrival in the home lab.

**Table 1:** Location of CTD stations during cruises MSM 59/2 (INDEX 2016) and SO 259 (INDEX 2017).

| CTD station | Latitude [°S] | Longitude [°E] |
|---|---|---|
| Cruise MSM 59/2 in 2016 | | |
| 03 | 23.01 | 67.07 |
| 14 | 23.87 | 69.50 |
| 22 | 22.89 | 69.16 |
| 32 | 21.78 | 69.02 |
| 35 | 21.61 | 69.44 |
| 52 | 21.17 | 68.62 |
| 67 | 21.72 | 67.67 |
| Cruise SO 259 in 2017 | | |
| 01 | 2.98 | 77.16 |
| 03 | 8.81 | 75.67 |
| 05 | 15.08 | 74.05 |
| 07 | 20.36 | 69.75 |
| 11 | 20.67 | 69.32 |
| 15 | 20.96 | 68.92 |
| 45 | 23.91 | 69.56 |
| 49 | 26.05 | 70.84 |
| 60 | 27.78 | 73.92 |
| 99 | 27.01 | 72.40 |

Biogeosciences Discuss., https://doi.org/10.5194/bg-2018-511
Manuscript under review for journal Biogeosciences
Discussion started: 3 January 2019


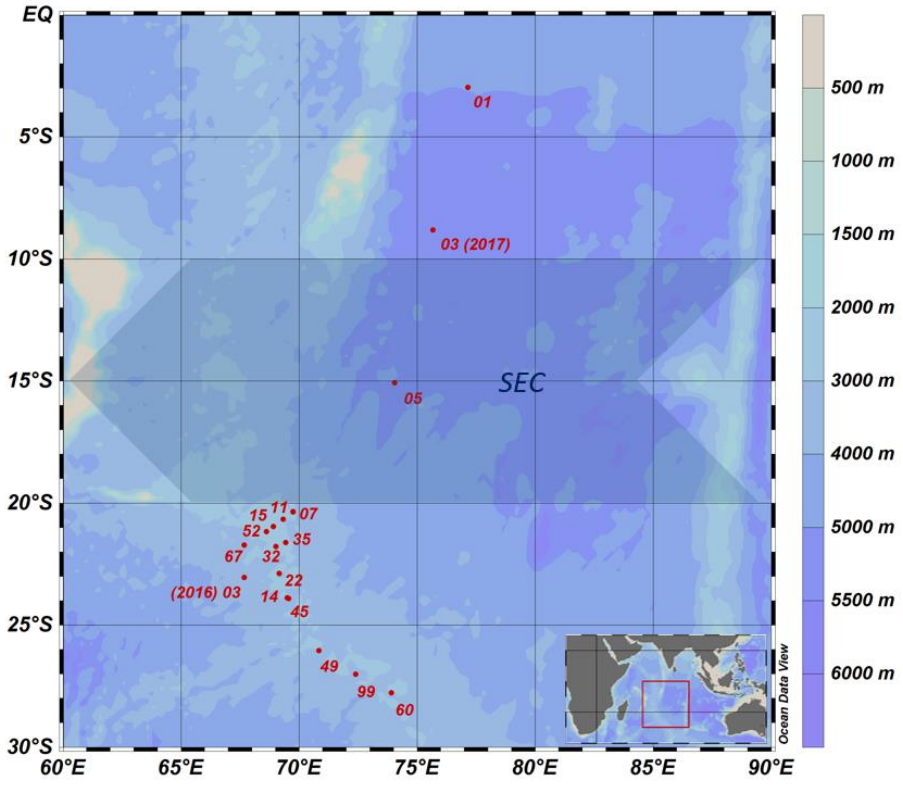


**Figure 1:** Sampling location during the cruises MSM 59/2 (INDEX 2016-2) and SO 259 (INDEX 2017). Shaded arrow represents the westward-directed, broad South Equatorial Current (SEC) after Woodberry (1989) from 10−20°S. Colors denote water depths.

## 2.2 Nutrient analyses

Nutrient concentrations (NOx, $NO_2^-$, $NH_4^+$, $PO_4^{3-}$) were measured with a SEAL AutoAnalyzer3HR with standard colorimetric methods (Grasshoff et al., 2009). Ammonia and nitrite concentrations were below detection limit. Nitrate determination included reduction of nitrate to nitrite with a cadmium reduction column. Nitrite ions reacted with sulphanilamide to form a diazo compound, followed by a reaction to an azo dye with N-(1-naphtyl-)ethylenediamine (NEDD) and was measured at 520−560 nm. Phosphate determination followed the method of Murphy and Riley (1962). Under acid conditions a phosphomolybdic complex was formed of ortho- phosphate, antimony and molybdate ion (Wurl 2009). Followed by reduction of ascorbic acid, the blue color complex was measured at 880 nm. The relative error of duplicate sample measurements was below 1.5 % for nitrate and phosphate concentrations and detection limit was <0.5 µM for NOx, and >0.1 µM for $PO_4^{3-}$.

Biogeosciences Discuss., https://doi.org/10.5194/bg-2018-511
Manuscript under review for journal Biogeosciences
Discussion started: 3 January 2019


### 2.3 Measurements of N and O isotopes of nitrate

Isotope measurements were only conducted for samples with nitrate concentrations >1.7 µM. Stable isotopes of nitrate ($\delta^{15}N$ and $\delta^{18}O$) were determined using the "denitrifier" method (Casciotti et al., 2002; Sigman and Casciotti, 2001). Nitrate and nitrite are converted to $N_2O$ gas using denitrifying bacteria (*Pseudomonas aureofaciens*). Based on nitrate concentrations, sample volumes were adjusted to yield 10 nmoles $N_2O$ and were injected into suspensions of *Pseudomonas aureofaciens* (ATCC#13985) for combined analysis of $\delta^{15}N$ and $\delta^{18}O$. The resulting $N_2O$ gas in headspace was purged into a GasBench II (ThermoFinnigan), and analysed in a Delta Plus XP mass spectrometer. Isotope ratios are reported in ‰ using the δ-notation:

$$\delta^{15}N = \left[\left(^{15}N/^{14}N_{sample}\right)/\left(^{15}N/^{14}N_{atm.N_2}\right) - 1\right] \times 1000 \quad (3)$$

$$\delta^{18}O = \left[\left(^{18}O/^{16}O_{sample}\right)/\left(^{18}O/^{16}O_{VSMOW}\right) - 1\right] \times 1000, \quad (4)$$

with air $N_2$ and VSMOW as reference for $^{15}N/^{14}N$ and $^{18}O/^{16}O$, respectively. The values were calibrated using IAEA-N3 ($\delta^{15}N$-$NO_3^-$ = +4.7 ‰ and $\delta^{18}O$-$NO_3^-$ = +25.6 ‰) and USGS-34 ($\delta^{15}N$-$NO_3^-$ = −1.8 ‰ and $\delta^{18}O$-$NO_3^-$ = −27.9 ‰ (Böhlke et al., 2003). A further internal potassium nitrate standard was analysed within each run for quality assurance. Isotope values were corrected using the "bracketing scheme" from Sigman et al. (2009) for $\delta^{18}O$-$NO_3^-$ and the single point correction referred to IAEA-N3 for $\delta^{15}N$-$NO_3^-$. The standard deviation for IAEA-N3 was 0.2 ‰ for $\delta^{15}N$-$NO_3^-$ and 0.3 ‰ for $\delta^{18}O$-$NO_3^-$, which is within the same specification for $\delta^{15}N$-$NO_3^-$ and $\delta^{18}O$-$NO_3^-$ for at least duplicate measurements of the samples.

## 3 Results

### 3.1 Physical water column properties

South of 25° S the upper 170 m are characterized by an intense salinity maximum with values of >35.5 PSU (Fig. 2a). The salinity maximum is carried northwards and is subducted underneath the surface layer within a temperature range of 22−15°C and with a core density of σ=25.5 kg/m³ (~250 m). Further north (CTD 03, 2017; 8.81° S) at the same density level, the salinity is significantly lower and reveals values of 35.2 PSU. The northernmost station (CTD 01, 2017; 2.89°S) indicates again a slight increase in salinity (>35.3 PSU). Between 22° S and 10° S, less saline surface water (<35.1 PSU) lies above the density level of the salinity maximum with temperatures of >23°C and densities above 24.0 kg/m³ (<150 m). South of 15° S, directly underneath the salinity maximum an oxygen maximum with values of >4.7 ml/l occurs at a density range of 26.4−26.9 kg/m³ (250−750 m; Fig. 2b) and temperatures between 15°C and 8°C. The lower limit of the oxygen maximum coincides with a temperature level of 8−9°C at σ=26.9−27.0 kg/m³ and marks the permanent thermocline at a depth of ~750 m in the south and at a depth of ~500 m in the north. Oxygen concentrations decrease towards the north and fall below 2 ml/l at the northernmost stations (CTD 01, CTD 03; 2017). Below the permanent thermocline (<9°C), an absolute salinity minimum with values less than 34.6 PSU is found in the southern region (Fig. 2a), within a density range of 26.9−27.4 kg/m³ (core density σ=27.2 kg/m³), which is strongly diluted further north. In the southern equatorial Indian Ocean at CTD 01 an increase in salinity (>34.9 PSU;

σ=27.2 kg/m³) corresponds with reduced oxygen concentrations of <1.1 ml/l. Overall, low oxygen concentrations dominate the northern study area and extend to the sub-thermocline water masses at the southernmost stations (<3.5 ml/l; Fig. 2b).

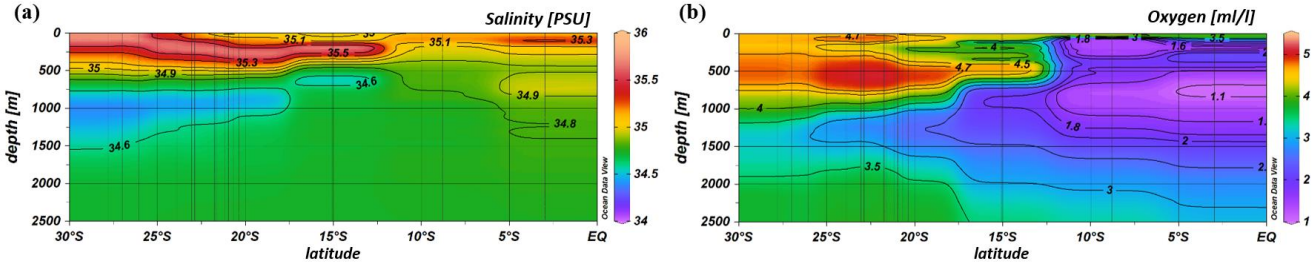


**Figure 2:** Profiles of salinity (a) and oxygen distribution (b) from CTD measurements during cruises MSM 59/2 (2016) and SO 259 (2017).

### 3.2 Nutrient concentration

The upper water column, in the depth range of the salinity maximum south of 20° S (<26.4 kg/m³), is strongly depleted in nitrate (~5.9 µM) and phosphate (<0.5 µM; Table 2). Nutrient concentrations rise within the oxygen maximum (σ= 26.4−26.9 kg/m³), where the nutrient concentrations reach values up to ~21 µM for nitrate and 1.5 µM for phosphate. Within the intermediate waters (~1000 m), nitrate and phosphate concentrations attain typical deep-sea values of >30 µM and >2 µM (Gruber and Sarmiento, 2006). Across the northern fringe of the gyre, at CTD 05 (2017; 15.08° S), nutrient concentrations slightly increase (Table 2).

Further north, at stations CTD 01 and 03, nutrient concentrations in the upper water column reach values typical for open ocean areas that are unaffected by gyral downwelling or high biological production. At 90 m water depth, concentrations were ~11 µM for nitrate and ~1 µM for phosphate (Table 2). Within the thermocline (<27. kg/m³; <550 m), nutrient concentrations attain values of >28 µM for nitrate and >2 µM for phosphate, before they level out at values of >35 µM for nitrate and >2.5 µM for phosphate at greater depth.

**Table 2:** Nitrate and phosphate concentrations summarized for CTD stations within the subtropical gyre (27.78°S−20.96°S), at the northern fringe (15.08°S) and north of the gyre (8.81°S−2.98°S). Samples were collected during cruises MSM 59/2 (INDEX 2016-2) and SO 259 (INDEX 2017). Results in the same area are similar and shown together.

| Latitude [°S] | Sigma-theta [kg/m³] | Depth [m] | $NO_3^-$[µM] | $PO_4^{3-}$[µM] |
|---|---|---|---|---|
| 27.78−20.96 | 26.4 | 310 | 5.9 | 0.5 |
| | 26.9 | 770 | 21.2 | 1.5 |
| | 27.4 | 1210 | 31.6 | 2.3 |
| 15.08 | 26.6 | 300 | 7.7 | 0.5 |
| | 26.9 | 550 | 22.7 | 1.6 |
| | 27.4 | 900 | 36.0 | 2.6 |
| 8.81−2.98 | 24.0 | 90 | 11.1 | 0.8 |
| | 27.0 | 550 | 28.2 | 2.0 |
| | 27.3 | 850 | 38.0 | 2.7 |

Biogeosciences Discuss., https://doi.org/10.5194/bg-2018-511
Manuscript under review for journal Biogeosciences
Discussion started: 3 January 2019


### 3.3 N and O isotopes of nitrate

In the upper 700 m, distinct N and O isotope maxima with $\delta^{15}N$ of >7.0 ‰ and $\delta^{18}O$ of >4.0 ‰ are found at latitudes 27.78° S–15.08° S (Table 3). This maximum is centred at ~400–500 m and correlates with the oxygen maximum of >4.7 ml/l. Between latitudes 23.91° S and 20.96° S, the N isotope maximum is observed at 400 m and the O isotope maximum is observed at 500 m, so that the isotope maxima are offset by ~100 m (Table 3). Above the isotopic maximum, both $\delta^{15}N$ and $\delta^{18}O$ decrease to values of ~5.4 ‰ and ~2.1 ‰, respectively, in the upper 300 m; an exception are the southernmost stations (CTD 49, 60, 99; 2017), where the elevated isotope values extend up to the surface.

In surface waters further north (<250 m), $\delta^{15}N$ and $\delta^{18}O$ increase to values of >7.0 ‰ and >4 ‰, respectively, at the northernmost station (CTD 01, 2017). Underneath this surface layer, N and O isotope ratios slightly decrease at ~180 m, before $\delta^{15}N$ and $\delta^{18}O$ again rise to >7.0 ‰ and >3.0 ‰, with an extended maximum in the depth interval from 300 m to 900 m that coincides with elevated salinities. Below the isotopic maxima in the southern region at ~400–500 m, and below the depth interval with high δ-values in the northernmost CTD station, $\delta^{15}N$ and $\delta^{18}O$ decrease towards deeper waters and have average values of 5.8 ‰ and 2.3 ‰ (Table 3).

**Table 3:** Average isotopic composition of nitrate in the surface layer, within the thermocline and in intermediate and deep waters of all CTD stations during cruises MSM 59/2 (INDEX 2016-2) and SO 259 (INDEX 2017). Data are combined for latitude sections (2.98–8.81° S, 15.08° S, 20.96–23.91° S and 26.05–27.78° S) that have similar isotopic composition. [a] $\delta^{15}N$ and $\delta^{18}O$ maxima. [b]Water depth of isotopic maxima. Results in the same area are similar and shown together.

| Latitude [°S] | Depth [m] | $\delta^{15}N$ [‰] | | $\delta^{18}O$ [‰] | |
|---|---|---|---|---|---|
| 27.78–26.05 | <700 | 7.3 | *7.8 [a] (200)[b]* | 4.1 | *5.0 [a] (370)[b]* |
| | 800-1200 | 6.3 | | 3.0 | |
| | 1300->3000 | 5.7 | | 2.2 | |
| 23.91–20.96 | <300 | 5.4 | | 2.1 | |
| | 300-650 | 7.3 | *7.7 [a] (400)[b]* | 4.5 | *5.0 [a] (500)[b]* |
| | 800-1000 | 6.2 | | 2.1 | |
| | 1500->3000 | 5.5 | | 1.6 | |
| 15.08 | <500 | 7.2 | *7.6 [a] (430)[b]* | 4.0 | *4.6 [a] (400)[b]* |
| | 600-800 | 6.6 | | 2.8 | |
| | 900->5000 | 6.0 | | 3.1 | |
| 8.81–2.98 | <85 | 7.3 | | 4.9 | |
| | 100-250 | 6.3 | | 3.3 | |
| | 300-850 | 7.0 | | 2.8 | |
| | 950-1150 | 6.7 | | 2.7 | |
| | 1250->5000 | 5.9 | | 2.4 | |

Biogeosciences Discuss., https://doi.org/10.5194/bg-2018-511
Manuscript under review for journal Biogeosciences
Discussion started: 3 January 2019




## 4 Discussion

### 4.1 Water mass distribution

Water masses in the working area are well discernible by their densities, salinities and oxygen concentrations (Fig. 3). In accordance with definitions from the literature, we identified water masses from the IOSG towards the southern equatorial Indian Ocean. We present the provenance of water masses of Antarctic and Subantarctic origin converging and mixing with water masses from the southern equatorial Indian Ocean and the Arabian Sea. The water mass distribution model is depicted in Fig. 4, which serves as a basis for the understanding of our nutrient and coupled N and O isotope measurements of nitrate.

#### 4.1.1 Surface and thermocline waters (<26.9 kg/m³; <800 m)

A high salinity surface layer (>35.5 PSU) centred at ~25.4 kg/m³ (Fig. 3a) is described in several studies. It has been termed "southern subtropical surface water" by Muromtsev (1959), "subtropical surface water" by Wyrtki (1973) and "subtropical subsurface water" (SSW) by Schott and McCreary (2001). For further descriptions, we adopt the definition of Wyrtki (1973) and use the abbreviation SSW. The SSW is formed in the subtropical gyre of the southern hemisphere by excess of evaporation over precipitation (Schott and McCreary, 2001) at latitudes 25−35° S (Baumgartner and Reichel, 1975). It is subducted into the thermocline of the subtropical gyre (Schott and McCreary, 2001), is detectable as far north as 15.08° S at CTD 05 (Fig. 3b) and not discernable further north in the southern equatorial Indian Ocean (Figs. 3c, 4).

Less saline surface water (<35.1 PSU) occurs above the density level of the salinity maximum (>23°C; <24.0 kg/m³; Fig. 3b) and is described by Wyrtki (1971) and Warren (1981). These low salinity values reflect an excess of precipitation over evaporation at latitudes 0−10° S (Baumgartner and Reichel, 1975) accompanied by the influx of low salinity water (34.0−34.5 PSU) from the Pacific Ocean through the Indonesian Archipelago, called "Indonesian Throughflow" (ITF). The ITF carries less saline water westwards by the SEC within the entire thermocline (Wyrtki, 1971; You and Tomczak, 1993). Emery (2001) named this less saline surface water (34.4−35.0 PSU) "Indonesian Upper Water" (IUW; Fig. 4).

The oxygen maximum south of 20° S in a density range of 26.4−26.9 kg/m³ (250−750 m; Fig. 3d) corresponds with the "Subantarctic Mode Water" (SAMW; Figs. 3, 4), described by McCartney (1977). It is formed at latitudes 40° S−50° S and injects oxygen saturated waters at a temperature range of 6−14°C into the subtropical gyre. On the transition to the north, the oxygen concentrations rapidly decrease from >4.6 ml/l (CTD 05; Fig. 3e) to <1.9 ml/l (CTD 01, 03; Fig. 3f) because of the absence of effective ventilation in the northern Indian Ocean. The reduced vertical changes in salinity north of ~15°S mark the "Indian Equatorial Water" (IEW; Fig. 4). This is described by Sharma (1976), Warren (1981), Quadfasel and Schott (1982), You and Tomczak (1993) and Schott and McCreary (2001) as a mixture of thermocline water masses from the northern and southern Indian Ocean.

#### 4.1.2 Intermediate water masses (26.9−27.3 kg/m³; 800−1000 m)

The salinity minimum (<34.9 PSU) south of 15° S, in a density range of 26.9−27.4 kg/m³ (core density σ=27.2 kg/m³; Fig. 3a) is associated with the "Antarctic Intermediate Water" (AAIW; Fig.4; Bindoff and McDougall, 2000; Deacon, 1933; Fine, 1993; Schott and McCreary, 2001; Toole and Warren, 1993; Warren, 1981; Wyrtki, 1973; You, 1998). It is transported eastwards by the "Antarctic Circumpolar Current" (ACC), penetrates into all three oceans and extends towards the equator to feed the intermediate waters (Fine, 1993; McCartney, 1977; Piola and Gordon, 1989; Reid, 1986, 1989; Sverdrup et al., 1942; Talley, 1996; Wüst, 1935).

The salinity minimum (<34.6 PSU) observed at station CTD 05 (15.08° S; Fig. 3b) has a slightly divergent core density (27.0 kg/m³) compared to the AAIW (Fig. 3a). This implies a further source to the salinity minimum of the AAIW. A low salinity water mass (~34.8 PSU) flows along 10−15° S (Schott and McCreary, 2001; Wyrtki, 1971; You and Tomczak, 1993) and originates from the ITF. At intermediate depths it has been called "Indonesian Intermediate Water" (IIW; Fig. 4) by Emery and Meincke (1986) and Emery (2001).

The increase in salinity (>34.9 PSU; Fig. 3c) further north, at the same density level as the AAIW, is caused by the inflow of saline water from the Arabian Sea, mainly from the Red Sea outflow (Warren, 1981) and is additionally feed by the outflow of the Persian Gulf (Emery and Meincke, 1986). Therefore, this water mass is called "Red Sea-Persian Gulf Intermediate Water" (RSPGIW; Fig. 4). The RSPGIW is transported towards the equator and beyond to as far south as 10° S (You, 1998), recirculates in the tropical gyre, and creates the absolute oxygen minimum (<1.1 ml/l) caused by biological processes in the Arabian Sea (see Sect. 4.2.1).

#### 4.1.3 Deep water masses (>27.3 kg/m³; >1000 m)

Overall low oxygen concentrations in the northern study area underneath the AAIW (>27.4 kg/m³; Fig. 3f) are caused by in situ consumption (Wyrtki, 1962) and reduced ventilation in the northern Indian Ocean. The deep oxygen minimum extends towards the south (~3.0 ml/l) and is associated with the water mass of the "Indian Deep Water" (IDW). The IDW has higher salinities than the overlying AAIW (Bindoff and McDougall, 2000; Mantyla and Reid, 1995; Schott and McCreary, 2001; Talley, 2013) with values of >34.6 PSU below the density range of the AAIW (Fig. 3a). The IDW (σ=~27.5 kg/m³) flows in the density range just above the "Circumpolar Deep Water" (CDW; Fig. 4) and a further increase in the salinity (34.62−34.73 PSU) and a decrease of the oxygen minimum at the 2°C temperature level (Emery, 2001) marks the transition between the IDW and the underlying CDW.

Biogeosciences Discuss., https://doi.org/10.5194/bg-2018-511
Manuscript under review for journal Biogeosciences
Discussion started: 3 January 2019


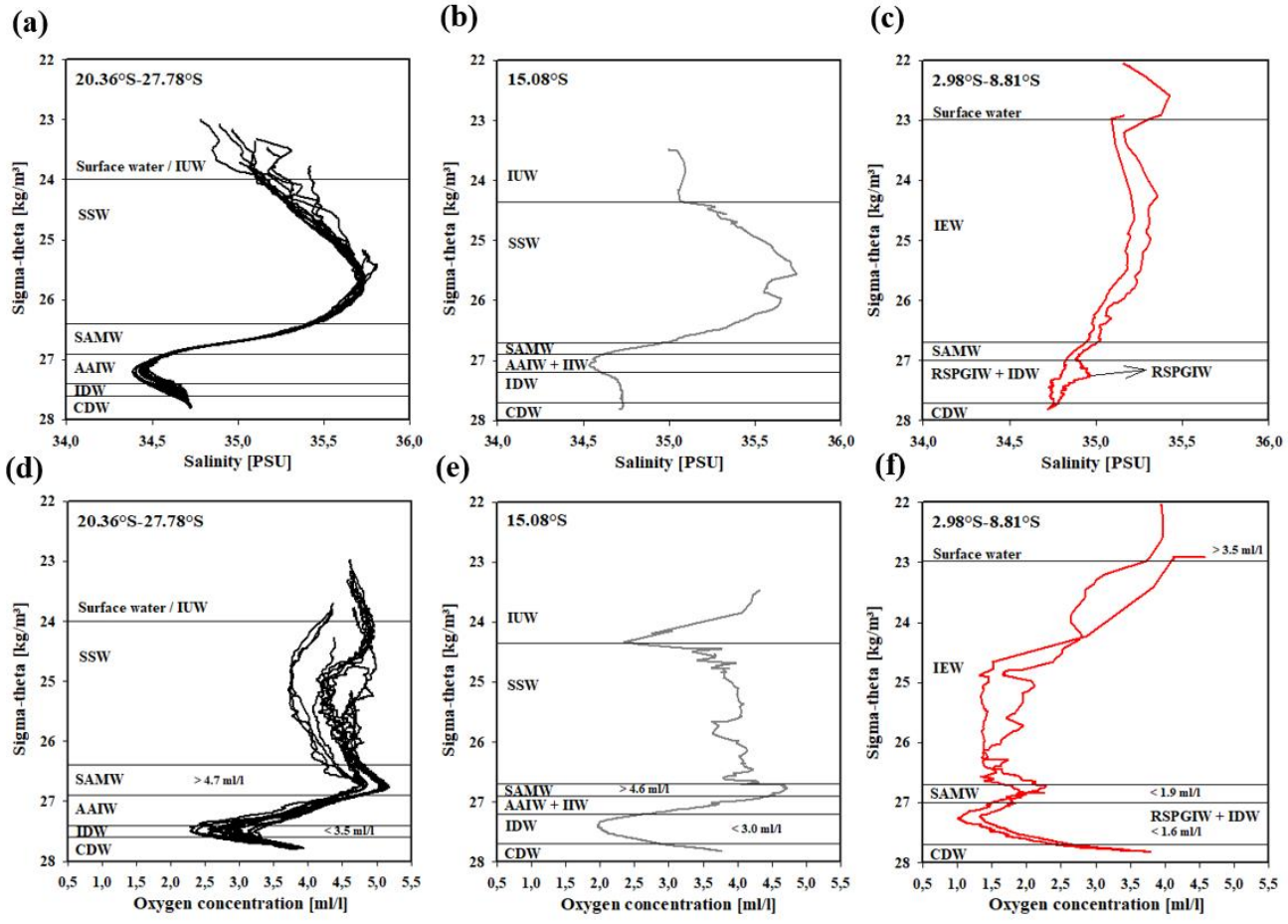


**Figure 3:** Water mass properties represented as salinity vs. sigma-theta diagrams (a, b, c) and as oxygen vs. sigma-theta diagrams (d, e, f) for CTD stations at latitudes 20.36° S−27.78° S, 15.08° S and 2.98° S−8.81° S.

Biogeosciences Discuss., https://doi.org/10.5194/bg-2018-511
Manuscript under review for journal Biogeosciences
Discussion started: 3 January 2019


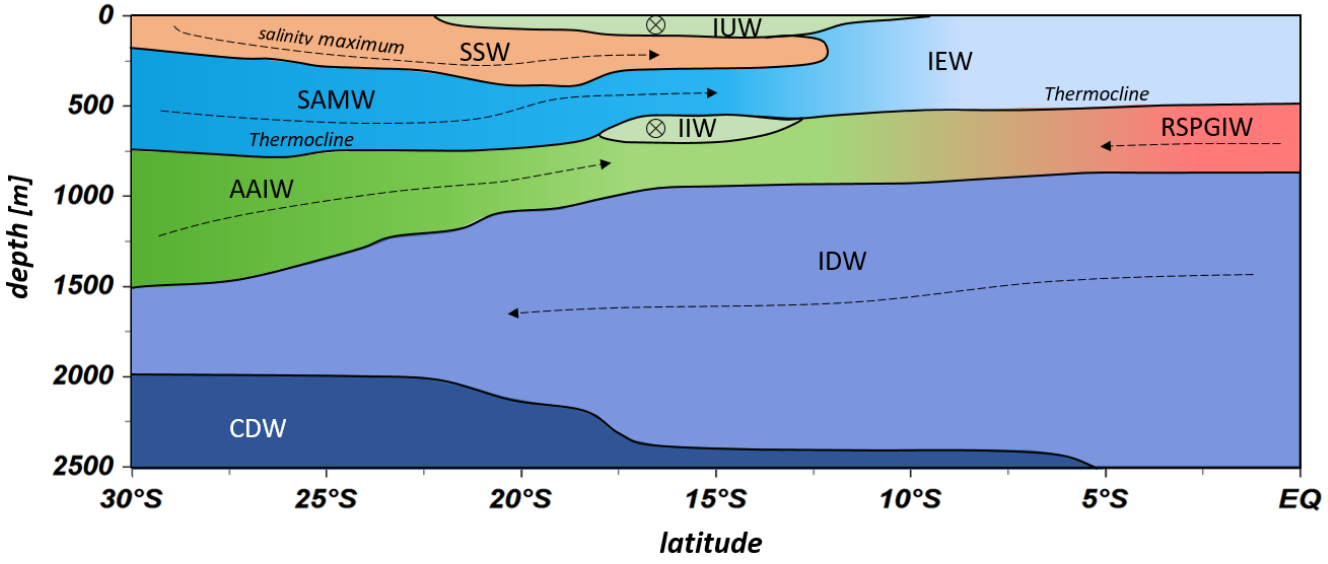


**Figure 4:** Water mass distribution model from 30° S to the equator. The CTD stations taken into account for this transect ranged between 67.07 °E and 77.16 °E. Indonesian Upper Water (IUW), Subtropical Surface Water (SSW), Subantarctic Mode Water (SAMW), Indian Equatorial Water (IEW), Antarctic Intermediate Water (AAIW), Indonesian Intermediate Water (IIW), Red Sea-Persian Gulf Intermediate Water (RSPGIW), Indian Deep Water (IDW), and Circumpolar Deep Water (CDW). Dotted lines represent N-S current directions and circled crosses indicate latitudinal directions from E to W.

### 4.2 Nutrient distribution and processes in the nitrogen cycle

#### 4.2.1 Nutrient supply in the oligotrophic subtropical gyre and lateral transfer across the gyre boundaries

Intense downwelling in the centre of the IOSG is induced by the convergence of horizontal Ekman volume flux (Williams and Follows, 2003) and creates the thick layer of nutrient depleted surface waters within the IUW and SSW (Fig. 5a, 5b), and also within the underlying SAMW. The northward increase in nutrients at ~15° S (CTD 05, 2017) marks the northern boundary of the subtropical gyre and the maximum extension of the IUW, SSW, and SAMW. Further increase in nutrient concentrations within the IEW indicate the transition from the subtropical gyre towards the southern equatorial Indian Ocean indicated by the characteristic shoaling of the nutricline at the northern fringe of the gyre.

The IEW is not a well-defined water mass, but rather a mixture of thermocline waters from the South Indian Ocean and from the nutrient-enriched northern Indian Ocean. Therefore, the nutrient concentrations increase towards the northernmost stations (CTD 01, 03; 2017) and indicate more and more influence of the nutrient-enriched northern Indian Ocean (Gaye et al., 2013). This increased northern influence is also reflected by the $NO_3^-/PO_4^{3-}$ ratios, which indicates values of less than 8 in the upper 200 m of the subtropical gyre and increase towards the southern equatorial Indian Ocean, tracking the outcropping nutriclines (Fig. 5c). Low $NO_3^-/PO_4^{3-}$ ratios are typical in surface waters of oligotrophic regions because nitrate commonly becomes depleted before phosphate (Gruber and Sarmiento, 2006; Deutsch et al., 2007).

Biogeosciences Discuss., https://doi.org/10.5194/bg-2018-511
Manuscript under review for journal Biogeosciences
Discussion started: 3 January 2019


Due to intense downwelling in the centre of the IOSG, the supply of nutrients by vertical mixing is reduced or absent in the gyre (Williams and Follows, 1998). Therefore, lateral transfer across the gyre boundaries and biologically induced in situ processes (e.g. $N_2$-Fixation) are the major processes supplying nutrients to the euphotic zone of the subtropical gyre.

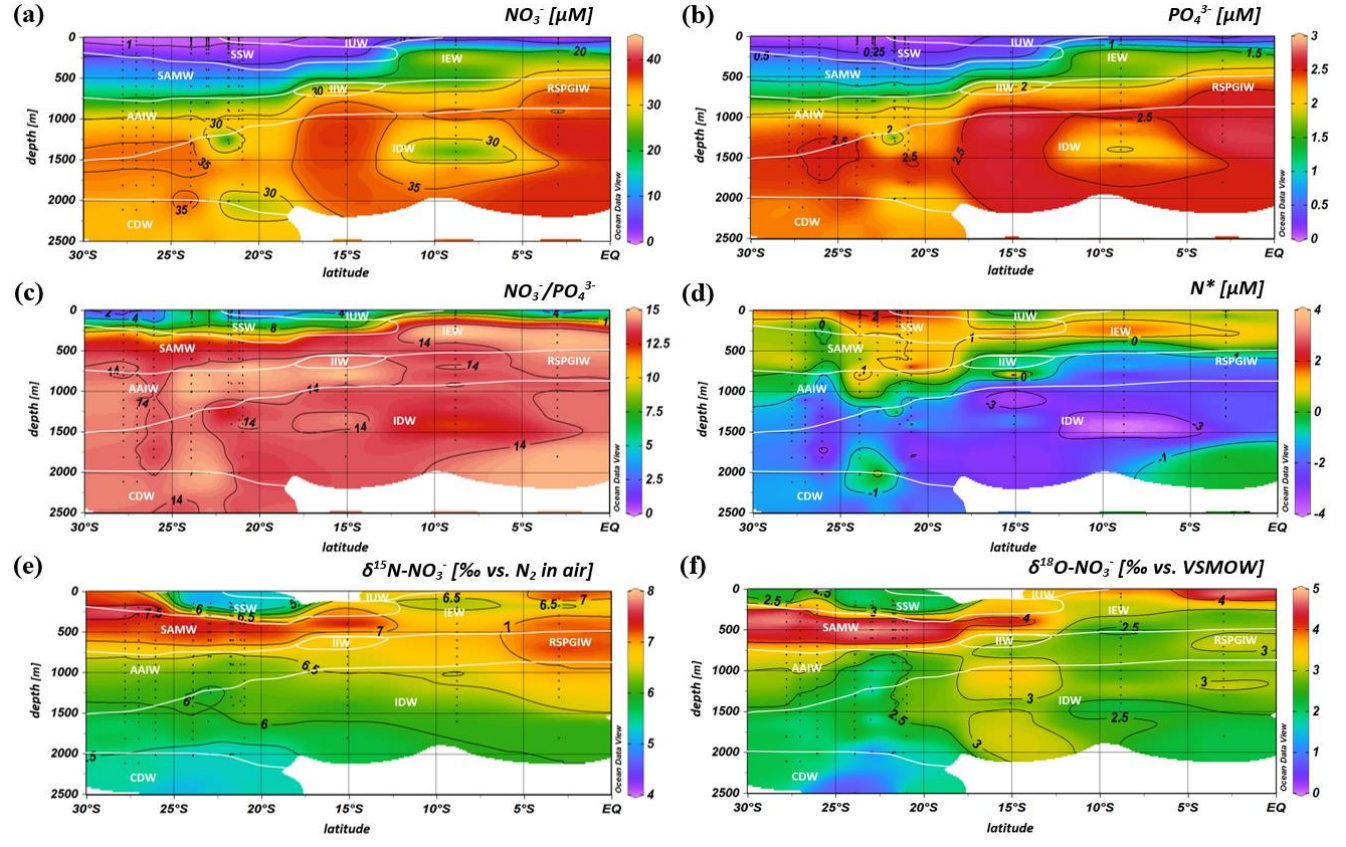


**Figure 5:** Profiles from south to north with an overlay of the water mass distribution (white contour lines) in the South Indian Ocean of nitrate (a) and phosphate concentrations (b), $NO_3^-/PO_4^{3-}$ ratio (c), N* (d), and $\delta^{15}N$ of nitrate (e) and $\delta^{18}O$ of nitrate (f).

The water masses entering the study area from the south and from the southern equatorial Indian Ocean have characteristic nutrient concentrations and isotope fingerprints of reactive nitrogen, so that some of the water masses are clearly discernible by the distribution of nutrients and the isotopic composition of nitrate within the IOSG. Our samples show $NO_3^-/PO_4^{3-}$ ratios of 14.56 on average (Fig. 6). These results differ from the global ocean mean of 16:1 (Redfield, 1934, 1963) and reveal a lower $NO_3^-/PO_4^{3-}$ ratio. Furthermore, measurements in the Arabian Sea reveal typical $NO_3^-/PO_4^{3-}$ ratios of ~12.81 (Codispoti et al., 2001), lower than our detected $NO_3^-/PO_4^{3-}$ ratios. Consequently, the average $NO_3^-/PO_4^{3-}$ ratio of 14.56 falls between the global ocean mean of 16:1 (Redfield, 1934, 1963) and the typical ratio in the Arabian Sea of ~12.81 (Codispoti et al., 2001). This alone indicates the mixing of water masses of southern and northern Indian Ocean origin.

Biogeosciences Discuss., https://doi.org/10.5194/bg-2018-511
Manuscript under review for journal Biogeosciences
Discussion started: 3 January 2019


The deviation from the Redfield stoichiometry (Bourbonnais et al., 2009; Redfield, 1934, 1963) is quantified by the tracer N* (Eq. 1). The Arabian Sea is characterised by an extensive oxygen deficit zone (ODZ) that induces denitrification in mid-water depths (Gaye et al., 2013) and leads to an N deficit in the water column (e.g., Bange et al., 2005; Rixen et al., 2005; Gaye et al., 2013). A deficit of N is expressed by a negative N* that in our data set has values of about −1 µM within the RSPGIW and values lower than −4 µM within the IDW (Fig. 5d).

These negative N* values are imported to intermediate and deep waters within the subtropical gyre and coincide with the oxygen minimum (see Sect. 4.1). Consequently, negative N* values are a result of the influx of water masses from the Arabian Sea.

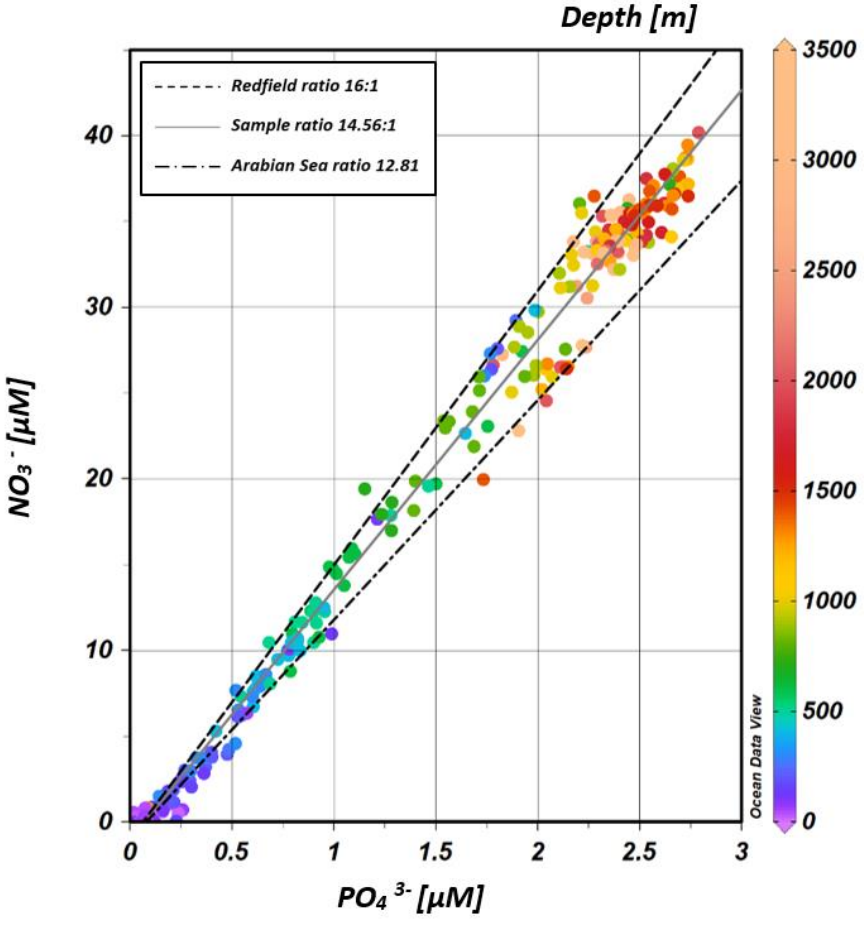


**Figure 6:** Correlation of nitrate versus phosphate concentrations. Regression line of the sample pool (solid, grey line) indicates a ratio of ~14.56, intermediate between the Redfield ratio of 16:1 (black, dashes line) and the mean ratio in the Arabian Sea with a slope of ~12.81 (grey, dotted-dashed line) after Codispoti et al. (2001). Color-coding of dots indicates the potential density Sigma-theta in kg/m³.

Biogeosciences Discuss., https://doi.org/10.5194/bg-2018-511
Manuscript under review for journal Biogeosciences
Discussion started: 3 January 2019


The denitrification signal, transported by the RSPGIW and IDW into the IOSG, is also detected in isotope signatures. Denitrification discriminates against the heavier isotope of nitrate ($^{15}N$, $^{18}O$), and raises $\delta^{15}N$ and $\delta^{18}O$ in equal proportions. Our measurements indicate elevated $\delta^{15}N$ and $\delta^{18}O$ values of >7 ‰ and >3 ‰ within the RSPGIW at CTD 01 and 03 (Fig. 5e, 5f) accompanied by nitrate concentrations of >30 µM (Fig. 5a). The significant progressive reduction of $\delta^{15}N$ and $\delta^{18}O$ towards the south to the IOSG is a result of mixing with other water masses contributing to the IEW and of respiration of relatively more $^{15}N$ depleted organic matter along the flow path.

Within the IOSG, $\delta^{15}N$ and $\delta^{18}O$ are also elevated within the SAMW (400−500 m) with values of >7 ‰ and >4 ‰ (Fig. 5e, 5f). However, compared with the RSPGIW, this pool has distinctly lower nitrate concentrations of <20 µM, which indicates another formation mechanism. The mechanism that elevated the isotope ratios in the SAMW is due to surface processes in the Subantarctic, where this water mass originates. In general, N-assimilation has an isotopic effect of about 5−10 ‰ (Montoya and McCarthy, 1995; Sigman et al., 2005; Waser et al., 1998) and produces biomass that is relatively depleted in $^{15}N$ and $^{18}O$ in comparison to the nitrate source. Consequently, this drives the elevation in $\delta^{15}N$ and $\delta^{18}O$ of the remaining nitrate as uptake proceeds. In oligotrophic waters, such as in the IOSG this isotopic effect is not expressed (Montoya et al., 2002), as nitrate is typically drawn down to the limit of detection by complete N-assimilation. Therefore, the elevated isotope values in the SAMW are a transport signal from the Subantarctic region and not a result of in situ processes in the gyre.

Nitrate in surface waters of the Southern Ocean is only partially assimilated due to light limitation (DiFiore et al., 2006; DiFiore et al., 2010; Sigman et al., 1999) and when this surface water is subducted, its nitrate pool has typical $\delta^{15}N$ values of ~5−9 ‰ (Sigman et al., 1999). This isotope trace of incomplete assimilation causes the elevated isotope values within the SAMW that enters the subtropical Indian Ocean thermocline with $\delta^{15}N$ values of >7 ‰ from the Southern Ocean (Table 3; Figs. 5e, 7a).

Biogeosciences Discuss., https://doi.org/10.5194/bg-2018-511
Manuscript under review for journal Biogeosciences
Discussion started: 3 January 2019


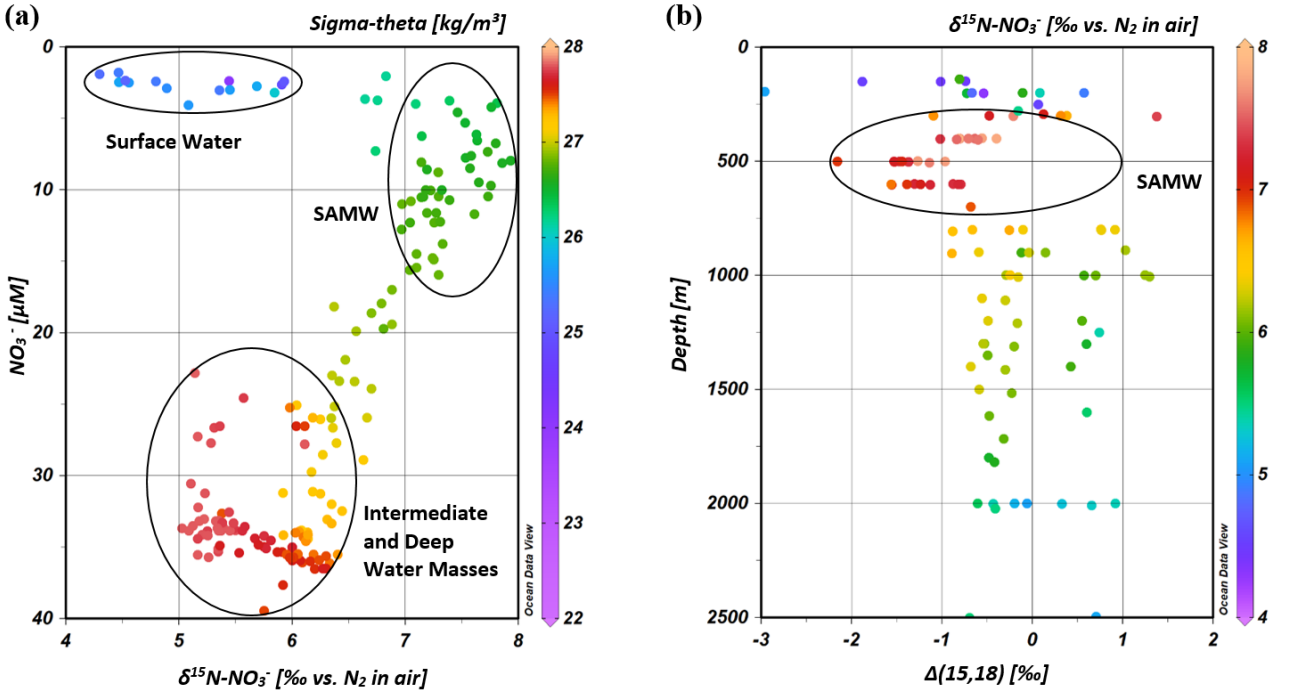


**Figure 7:** Nitrate concentrations versus $\delta^{15}N$ of nitrate for CTD stations within the IOSG (a). Color-code of dots indicates the potential density sigma-theta (kg/m³). Figure 7b represents the tracer Δ(15,18) versus water depth, where colored dots are the $\delta^{15}N$ of nitrate for CTD stations between 17° S and 25 °S.

The nitrate isotope properties match measurements in the Southern Ocean south of 40° S by Sigman et al. (1999, 2000) and DiFiore et al. (2006). They use the correlation of $\delta^{15}N$ and the fraction of nitrate remaining - $\ln(NO_3^-)$ - to quantify the isotope fractionation effect during N-uptake in the Antarctic and Subantarctic region. If N-uptake occurs with a constant effect and no new nitrate is added to the surface ocean, then the uptake process can be described in terms of Rayleigh fractionation kinetics (Mariotti et al., 1981). To fulfil the conditions of Rayleigh fractionation, the nitrate samples plot along a straight line in $\delta^{15}N/\ln(NO_3)$ space, where the slope of the line represents the isotope effect of N-uptake or mixing of different nitrate pools. Sigman et al. (1999, 2000) and DiFiore et al. (2006) compare the theoretically Rayleigh utilization trend of $\delta^{15}N/\ln(NO_3)$=5 ‰ with their measured nitrate utilisation trend within the Subantarctic thermocline, where Sigman et al., (1999, 2000) determined a slope of $\delta^{15}N/\ln(NO_3)$~1.3 ‰ (Fig. 8).

Subantarctic thermocline waters are the source water of the SAMW and the underlying AAIW in the IOSG. Our results reveal a similar nitrate utilization signal with a slightly shallower regression line of $\delta^{15}N/\ln(NO_3)$~0.93 ‰ (Fig. 8). It is clearly a mixing signal that causes the moderate slopes of $\delta^{15}N/\ln(NO_3)$ in both the gyre region and in the Subantarctic because biological utilisation of nitrate is unlikely. The explanation for the slightly shallower slope in our data set compared to the

results in the Subantarctic is vertical mixing with the overlying SSW that has lower $\delta^{15}N$ values (<6 ‰) with nitrate concentrations of <5 µM and a fundamentally different formation background (Fig. 7a; see Sect. 4.2.2). Deep-water nitrate concentrations vary little and $\delta^{15}N$ increases towards lower water depths and the nitrate utilisation signal slightly differ from that of the Southern Ocean due to the influence of the IDW.

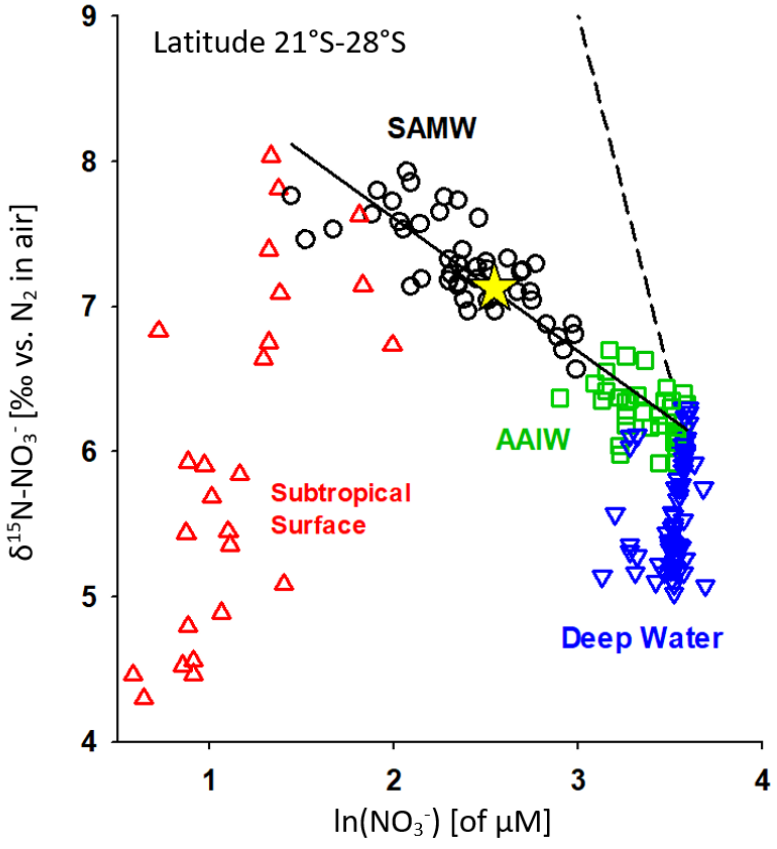


**Figure 8:** The $\delta^{15}N$ of nitrate versus $\ln(NO_3^-)$ for CTD stations at latitude 21° S–28° S. Data were grouped for the subtropical surface, SAMW, AAIW and deep water. The regression line of samples within the SAMW and AAIW (solid line) is similar to that in the Subantarctic thermocline (Sigman et al., 1999, 2000). The dashed line illustrates the Rayleigh nitrate utilization trend with a slope of 5 ‰. The yellow star marks the mean $\delta^{15}N$ of nitrate (7.1 ‰) and $NO_3^-$ (12.8 µM) of SAMW in the Subantarctic region after DiFiore et al. (2006).

Within the isotope maxima of the SAWM (~500 m), the uniform evolution of N and O isotopes of nitrate breaks down, accompanied by an offset (~100 m) of the depths of the isotopic maxima at 23.91° S–20.36° S (Table 3). Both, $\delta^{15}N$ and $\delta^{18}O$, are elevated within the SAMW, but $\delta^{15}N$ is less elevated than $\delta^{18}O$. The decoupling of N and O isotopes is expressed by the tracer $\Delta(15,18)$ (see Eq. 2) that is sensitive with regard to source signatures. Therefore, we adopt the CDW as the source water

and source nitrate pool ($\delta^{15}N_{deep}$=5.5 ‰; $\delta^{18}O_{deep}$=1.7 ‰) for the subtropical region. Consequently, less elevation of $\delta^{15}N$ compared to $\delta^{18}O$ leads to a negative Δ(15,18).

Negative Δ(15,18) values of <−0.5 ‰ (Fig. 7b) arise within the SAMW and may be an indirect effect of the partial N-assimilation in the Subantarctic. Isotope fractionation during the initial phase of partial N-assimilation leads to sinking organic matter that is more depleted in $^{15}N$ than the source nitrate (Sigman et al., 1999; Rafter et al., 2013). Remineralization of this sinking organic matter adds nitrate that is depleted in $^{15}N$ and lowers $\delta^{15}N$ of the ambient nitrate and thus leads to a negative Δ(15,18) from the N-isotope side. To conclude, remineralization of organic matter produced by partial N-assimilation in the Southern Ocean indicates a negative Δ(15,18) and leads to the deviation of the isotope maxima with an offset of 100 m within the depth range of the SAMW. However, the remineralization of $^{15}N$-depleted organic matter formed out of newly fixed N from $N_2$-fixation in surface waters may also drives the decrease of Δ(15,18) (see the following Sect. 4.2.2).

#### 4.2.2 N2-fixation in the SIOG

The mixing of source water signals from the lateral influx of the neighbouring northern Indian Ocean and Southern Ocean are important influences on nutrient distribution and isotopic composition of nitrate in the gyre region. However, N* and $\delta^{15}N$ also suggest that $N_2$-fixation is an important process within the IOSG and introduces new nitrate into the surface waters. The N* increased up to 1.5−2 µM at 60−200 m and is an evidence for the input of newly fixed N that shifts the $NO_3^-/PO_4^{3-}$ ratio from the Redfield stoichiometry to higher ratios (Bourbonnais et al., 2009; Redfield, 1934, 1963). Such shifts also have been attributed to preferential remineralization of N over P and results in an overestimation of N*. However, a first order driver of positive N* clearly is $N_2$-fixation (Bourbonnais et al., 2009; Monteiro and Follows, 2006).

We use $\delta^{15}N$ and $\delta^{18}O$ of nitrate as additional indicators of N sources to overcome the weakness associated with the N* approach. $N_2$-fixation produces organic matter that has a low $\delta^{15}N$ relative to average oceanic combined nitrogen (Carpenter et al., 1997; Minagawa and Wada, 1986; Montoya et al., 2002; Wada and Hattori, 1976). Within the surface waters (<250 m) of the IOSG (~17° S−25° S), the $\delta^{15}N$ of nitrate is lower than 5.5 ‰ (Figs. 5e, 7a). Although this δ-value is high compared to other regions of intense $N_2$-fixation, such as in the oligotrophic North Atlantic, where values near −1 to −2 ‰ are common (Montoya et al., 2002), contradict the assumption of $N_2$-fixation in surface waters within the IOSG. However, considering SAMW and SSW as the sources for injection of nutrients into the gyre with elevated $\delta^{15}N$ values of >7.0 (~17° S−25° S), $\delta^{15}N$ is clearly reduced in surface waters. This indicates an addition of isotopically light N from the atmosphere in the gyre region from 17° S to 25° S (Fig. 7a).

Furthermore, $\delta^{18}O$ indicates values of <3 ‰ and shows a minor decrease compared to $\delta^{15}N$. This decoupling of N and O isotopes of nitrate again leads to a negative Δ(15,18), a typical indicator of $N_2$-fixation. Several lines of evidence thus show that $N_2$-fixation occurs in the subtropical gyre: the negative Δ(15,18) of <−0.5 ‰ down to 250 m (Fig. 7b), accompanied by distingtly low $\delta^{15}N$ (Fig. 5e), and elevated N* of >1 µM (Fig. 5d). These, and the distance from any external nitrate sources are unambiguous evidences of diazotrophic activity within the surface layer.

Biogeosciences Discuss., https://doi.org/10.5194/bg-2018-511
Manuscript under review for journal Biogeosciences
Discussion started: 3 January 2019


To estimate the supply of newly fixed N to the nutrient pool, we calculate the fraction of nitrate coming from $N_2$-fixation with the following equation:

$$NO_3^-/PO_4^{3-}{}_{cal} = NO_3^-{}_{sample}/(\frac{NO_3^-{}_{in}}{NO_3^-/PO_4^{3-}{}_{in}} - \frac{NO_3^-{}_{ass}}{NO_3^-/PO_4^{3-}{}_{ass}}) \quad (5)$$

with "$NO_3^-{}_{in}$" as initial nitrate concentration of the source water (SAMW within the IOSG and IEW in the southern equatorial region), "$NO_3^-{}_{ass}$" denoting the assimilated nitrate ($NO_3^-{}_{in}$–$NO_3^-{}_{sample}$) and "$NO_3^-{}_{sample}$" being the sample concentrations. The initial nitrate to phosphate pool $NO_3^-/PO_4^{3-}{}_{in}$ is defined as mean ratio of the source water. For the region of the IOSG, we presume that the mean ratio within the SAMW is 13.25 and 14.25 in the southern equatorial Indian Ocean. For N-assimilation in the euphotic zone we assume Redfield conditions of $NO_3^-/PO_4^{3-}{}_{ass}$ = 16. To calculate the residual nitrate, we multiply the calculated nitrate to phosphate ratio ($NO_3^-/PO_4^{3-}{}_{cal}$) with the measured phosphate concentrations:

$$NO_3^-{}_{cal} = \frac{NO_3^-/PO_4^{3-}{}_{cal}}{PO_4^{3-}{}_{sample}} . \quad (6)$$

The difference of $NO_3^-{}_{sample}$ and $NO_3^-{}_{cal}$ represents the portion of the nitrate formed by nitrification out of newly fixed N, which is consumed by N-assimilation under Redfield conditions. At latitude 17° S–25° S, our samples indicate elevated $NO_3^-/PO_4^{3-}$ ratios and a resulting positive deviation from the calculated line of N-assimilation at nitrate concentrations of <10 µM (Fig. 9a). Consequently, $N_2$-fixation leads to the local elevation in $NO_3^-/PO_4^{3-}$ ratios due to the input of new N and coincide with the decrease of $\delta^{15}N$ and the decoupling of N and O isotopes, leading to a negative Δ(15,18). The quantity of newly fixed nitrate ($NO_3^-{}_{fix}$) is given by the formula

$$NO_3^-{}_{fix}\ [in\ \%] = \frac{(NO_3^-{}_{sample} - NO_3^-{}_{cal})}{NO_3^-{}_{sample}} * 100 \quad , \quad (7)$$

which is represented in Fig. 9b, indicating a distinct upward increase in the upper 200 m at 17° S–25° S with an average portion of fixed nitrate of about 34 %, suggesting that about one-third of the nitrate measured in the upper 200 m is derived from newly fixed nitrogen. Considering an average $\delta^{15}N$ of 7.3 ‰ of the source water (SAMW) and a $\delta^{15}N$ of 0 ‰ for the atmospheric $N_2$, we can calculate a $\delta^{15}N$-$NO_3^-{}_{fix}$ of ~4.8 ‰ in the surface water. Our measurements show an average $\delta^{15}N$ of ~5.1 ‰ in the upper 200 m with a minimum of 4.3 ‰ (CTD 52; 2016) and a maximum of 5.9 ‰ (CTD 32; 2016) and hence, agree with the calculated $\delta^{15}N$-$NO_3^-{}_{fix}$.

Biogeosciences Discuss., https://doi.org/10.5194/bg-2018-511
Manuscript under review for journal Biogeosciences
Discussion started: 3 January 2019


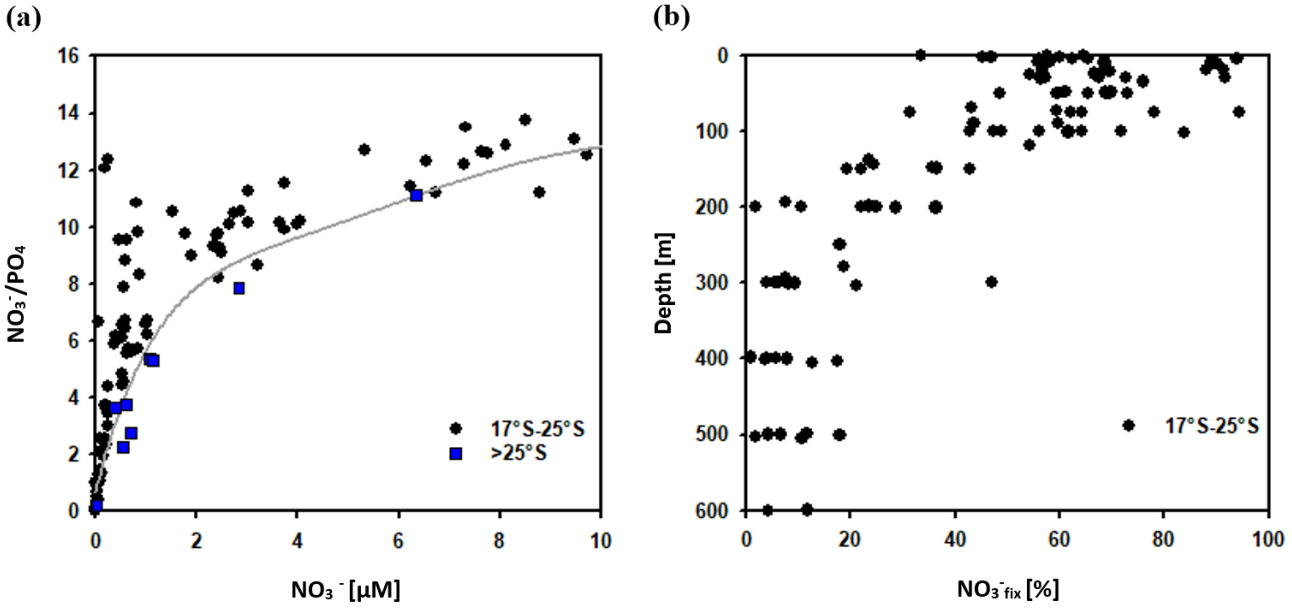


**Figure 9:** $NO_3^-/PO_4^{3-}$ ratio versus nitrate concentrations of seawater samples at 17° S–25° S and >25° S (a). The grey solid line indicates the calculated N-assimilation with a preformed $NO_3^-:PO_4^{3-}{}_{in}$ ratio of 13.25 for the region of the IOSG and 14.25 for the southern equatorial Indian Ocean and progressive nutrient assimilation with a Redfield ratio of 16 ($NO_3^-/PO_4^{3-}{}_{ass}$). In Fig. 9b we present the portion of nitrate formed out of newly fixed N ($NO_3^-{}_{fix}$) versus depth at latitudes 17° S–25° S.

Further south (>25° S), samples plot close to the line of N-assimilation and no significant input of fixed nitrate is indicated (Fig. 9a). This agrees with the $\delta^{15}N$ values in surface waters, indicating the same values as in the underlying SAMW (>7 ‰), while $\delta^{18}O$ shows low values of <3 ‰. Consequently, N and O isotopes show a counteracting behaviour that differs from the region at ~17° S–25° S, resulting in a positive Δ(15,18) of >0.5 ‰ (Fig. 5g). This is evidence for the absence of $N_2$-fixation in this region but also indicates that $\delta^{18}O$ remains low due to ongoing nitrate production by nitrification.

$N_2$-fixation in the tropical and subtropical oceans is restricted to areas with seawater temperatures in the range of 20–30°C (Capone et al., 1997; Breitbarth et al., 2007). Modelling $N_2$-fixation with this assumption thus resulted in very limited fixation south of about 25° S, although phosphate and iron are not limiting (Paulsen et al., 2017). At latitudes north of 25° S, where we see a significant contribution of $N_2$-fixation, surface temperatures exceed 20°C, and reach up to 29°C (S1). In comparison, south of 25° S, where $N_2$-fixation is not detectable, we observe sea surface temperatures of 20.5°C on average, and less than 20°C just below the surface. These lower temperatures can thus explain the absence of $N_2$-fixation south of 25° S.

## Conclusions

The subtropical gyre of the South Indian Ocean is one of five gyres in the world's oceans, which develop extensive oligotrophic regions. The South Indian Ocean gyre (IOSG) is the only oligotrophic gyre in the Indian Ocean due to the land-locked nature of the northern Indian Ocean. Compared to the Atlantic and Pacific Ocean gyres the IOSG is less explored and is poorly understood in terms of nutrient distribution and isotopic composition of nitrate.

This work compiles the general distribution of water masses from 30° S, within the IOSG, across the South Equatorial Current (SEC), and towards the southern equatorial Indian Ocean. The water mass distribution model provides a basis for the identification of nutrient sources and the isotopic signatures of nitrate, which are among the first reported in this region. Water masses in our study area are diverse and originate in two fundamentally different ocean regimes: In the Southern Ocean (SAMW and AAIW) and in the northern Indian Ocean (RSPGIW and IDW). These different water masses have a major influence on the nutrient distribution and stable isotope composition of nitrate.

The patterns demonstrate the lateral influx from the Arabian Sea, characterized by strong denitrification in mid-water depths that leads to an N deficit in intermediate and deep waters accompanied by elevated isotope ratios of nitrate within the RSPGIW. The lateral influx from the Southern Ocean is via the oxygen saturated SAMW, with characteristically elevated isotope ratios of nitrate due to partial N-assimilation in the high southern latitudes.

Additionally, the data mirror an external input of N by $N_2$-fixation that is indicated by positive N* and negative $\Delta(15,18)$ values in surface waters. In the upper 200 m of the region 17° S–25° S we calculate that approximately one-third of the nitrate consumed by N-assimilation is provided by from newly fixed nitrogen.

The IOSG has been sparsely investigated and is an area representing those oceanic oligotrophic regions that are likely to adjust to continued warming by deepening stratification, reduced upward nutrient supply across the thermocline, and decreasing biological production. Whether this will be offset by enhanced $N_2$-fixation in warming surface is an open question that needs dedicated follow-up studies, both in terms of experimental approaches, time series observation, remote sensing, and biogeochemical modelling.

*Data availability.* The data will be available in the data publisher PANGAEA.

*Author contribution.* N. Lahajnar and N. C. Harms collected the samples on board. U. Schwarz-Schampera conceived the INDEX program in the IOSG and lead the cruises. N. Lahajnar, B. Gaye, T. Rixen and K.-C. Emeis designed the nutrient and nitrogen cycle study. N. C. Harms, N. Lahajnar, K. Dähnke and M. Ankele participated in the sample analyses. N. C. Harms, N. Lahjnar and B. Gaye analysed the data. N. C. Harms wrote the first draft of the manuscript. All authors contributed substantially to the final paper

*Competing interests.* The authors declare that they have no conflict of interest.

*Acknowledgments.* Cruises and sampling were conducted in the INDEX program of the Federal Institute for Geosciences and Natural Resources (BGR). The INDEX program explores polymetallic sulfides on the ocean floor, based on a fifteen-year contract of BGR with the International Seabed Authority. BGR requests acknowledgment in any future use of the data and results in this publication. We thank the crew of the research vessels *Merian* and *Sonne* for supporting our work on board. Furthermore, we thank our colleagues, from the Helmholtz Institute, especially Tina Sanders, in Geesthacht for supporting our analyses of nutrients and stable isotopes of nitrate.

## References

Bange, H. W., Naqvi, S. W. A., and Codispoti, L.: The nitrogen cycle in the Arabian Sea. Prog. Oceanogr., 65(2-4), 145-158, https://doi.org/10.1016/j.pocean.2005.03.002, 2005.

Baumgartner, A., and Reichel, E.: The world water balance: Mean annual global, continental and maritime precipitation evaporation and run-off: Elsevier Science Inc, 1975.

Behrenfeld, M. J., O'Malley, R. T., Siegel, D. A., McClain, C. R., Sarmiento, J. L., Feldman, G. C., Milligan, A. J., Falkowski, P. G., Letelier, R. M., and Boss, E. S.: Climate-driven trends in contemporary ocean productivity. Nature, 444(7120), 752, 2006.

Bianchi, M., Feliatra, F., Tréguer, P., Vincendeau, M.-A., and Morvan, J.: Nitrification rates, ammonium and nitrate distribution in upper layers of the water column and in sediments of the Indian sector of the Southern Ocean. Deep-sea Res. Pt. II, 44(5), 1017-1032, https://doi.org/10.1016/S0967-0645(96)00109-9, 1997.

Bindoff, N. L., and McDougall, T. J.: Decadal changes along an Indian Ocean section at 32°S and their interpretation. J. Phys. Oceanogr., 30(6), 1207-1222, https://doi.org/10.1175/1520-0485(2000)030<1207:DCAAIO>2.0.CO;2, 2000.

Böhlke, J. K., Mroczkowski, S. J., and Coplen, T. B.: Oxygen isotopes in nitrate: new reference materials for 18O:17O:16O measurements and observations on nitrate-water equilibration. Rapid Commun. Mass Sp., 17(16), 1835-1846, https://doi.org/10.1002/rcm.1123, 2003.

Bourbonnais, A., Lehmann, M. F., Waniek, J. J., and Schulz-Bull, D. E.: Nitrate isotope anomalies reflect N2 fixation in the Azores Front region (subtropical NE Atlantic). J. Geophys. Res.-Oceans, 114(C3), n/a-n/a, https://doi.org/10.1029/2007JC004617, 2009.

Brandes, J. A., Devol, A. H., Yoshinari, T., Jayakumar, D. A., and Naqvi, S. W. A: Isotopic composition of nitrate in the central Arabian Sea and eastern tropical North Pacific: A tracer for mixing and nitrogen cycles. Limnol. Oceanogr., 43(7), 1680-1689, https://doi.org/10.4319/lo.1998.43.7.1680, 1998.

Breitbarth, E., Oschlies, A., and LaRoche, J.: Physiological constraints on the global distribution of Trichodesmium - effect of temperature on diazotrophy. Biogeosciences, 4(1), 53-61, 2007.

Capone, D. G., Zehr, J. P., Paerl, H. W., Bergman, B., and Carpenter, E. J.: Trichodesmium, a Globally Significant Marine Cyanobacterium. Science, 276(5316), 1221-1229, https://doi.org/10.1126/science.276.5316.1221, 1997.

Carpenter, E. J., Harvey, H. R., Fry, B., and Capone, D. G.: Biogeochemical tracers of the marine cyanobacterium Trichodesmium. Deep-Sea Res. Pt. I, 44(1), 27-38, https://doi.org/10.1016/S0967-0637(96)00091-X, 1997.

Casciotti, K. L., Sigman, D. M., Hastings, M. G., Böhlke, J., and Hilkert, A.: Measurement of the oxygen isotopic composition of nitrate in seawater and freshwater using the denitrifier method. Anal. Chem., 74(19), 4905-4912, https://doi.org/10.1021/ac020113w, 2002.

Clark, D. R., Rees, A. P., and Joint, I.: Ammonium regeneration and nitrification rates in the oligotrophic Atlantic Ocean: Implications for new production estimates. Limnol. Oceanogr., 53(1), 52-62, https://doi.org/10.4319/lo.2008.53.1.0052, 2008.

Codispoti, L., Brandes, J. A., Christensen, J., Devol, A., Naqvi, S., Paerl, H. W., and Yoshinari, T.: The oceanic fixed nitrogen and nitrous oxide budgets: Moving targets as we enter the anthropocene? Sci. Mar., 65(S2), 85-105, 2001.

Colborn, J. G.: The thermal structure of the Indian Ocean. University Press of Hawaii Honolulu, 1975.

Deacon, G. E.: A general account of the hydrology of the South Atlantic Ocean. Discovery Reports, 7, 171-238, 1933.

Deutsch, C., Gruber, N., Key, R. M., and L., S. J.: Denitrification and $N_2$ fixation in the Pacific Ocean. Global Biogeochem. Cy., 15(2), 483-506, https://doi.org/10.1029/2000GB001291, 2001.

Deutsch, C., Sarmiento, J. L., Sigman, D. M., Gruber, N., and Dunne, J. P.: Spatial coupling of nitrogen inputs and losses in the ocean. Nature, 445, 163, https://doi.org/10.1038/nature05392, 2007.

DiFiore, P. J., Sigman, D. M., Trull, T. W., Lourey, M. J., Karsh, K., Cane, G., and Ho, R.: Nitrogen isotope constraints on subantarctic biogeochemistry. J. Geophys. Res.-Oceans, 111(C8), n/a-n/a, https://doi.org/10.1029/2005JC003216, 2006.

DiFiore, P. J., Sigman D. M., Karsh Kristen, L., Trull Thomas, W., Dunbar Robert, B., and Robinson Rebecca, S. (2010). Poleward decrease in the isotope effect of nitrate assimilation across the Southern Ocean. Geophys. Res. Lett., 37(17), https://doi.org/10.1029/2010GL044090, 2010.

Duing, W.: The monsoon regime of the currents in the Indian Ocean: Hawaii inst of Geophysics Honolulu, 1970.

Emerson, S., Mecking, S., and Abell, J.: The biological pump in the subtropical North Pacific Ocean: Nutrient sources, Redfield ratios, and recent changes. Global Biogeochem. Cy., 15(3), 535-554, https://doi.org/10.1029/2000GB001320, 2001.

Emery, W. J.: Water types and water masses. Encyclopedia of ocean sciences, 6, 3179-3187, https://doi.org/10.1006/rwos.2001.0108, 2001.

Emery, W. J., and Meincke, J.: Global water masses: summary and review. Oceanologica Acta, 9, 383-391, 1986.

Fine, R. A.: Circulation of Antarctic intermediate water in the South Indian Ocean. Deep-Sea Res.h Pt. I, 40(10), 2021-2042, https://doi.org/10.1016/0967-0637(93)90043-3, 1993.

Gaye, B., Nagel, B., Dähnke, K., Rixen, T., and Emeis, K. C. (2013). Evidence of parallel denitrification and nitrite oxidation in the ODZ of the Arabian Sea from paired stable isotopes of nitrate and nitrite. Global Biogeochem. Cy., 27(4), 1059-1071, https://doi.org/10.1002/2011GB004115, 2013.

Gaye-Haake, B., Lahajnar, N., Emeis, K.-C., Unger, D., Rixen, T., Suthhof, A., Ramaswamy, V., Schulz, H., Paropkari, A., and Guptha, M.: Stable nitrogen isotopic ratios of sinking particles and sediments from the northern Indian Ocean. Mar. Chem., 96(3-4), 243-255, https://doi.org/10.1016/j.marchem.2005.02.001, 2005.

Godfrey, J., and Golding, T.: The Sverdrup relation in the Indian Ocean, and the effect of Pacific-Indian Ocean throughflow on Indian Ocean circulation and on the East Australian Current. J. Phys. Oceanogr., 11(6), 771-779, https://doi.org/10.1175/1520-0485(1981)011<0771:TSRITI>2.0.CO;2, 1981.

Granger, J., Sigman D. M., Needoba Joseph, A., and Harrison Paul, J.: Coupled nitrogen and oxygen isotope fractionation of nitrate during assimilation by cultures of marine phytoplankton. Limnol. Oceanogr., 49(5), 1763-1773, https://doi.org/10.4319/lo.2004.49.5.1763, 2004.

Grasshoff, K., Kremling, K., and Ehrhardt, M.: Methods of seawater analysis: John Wiley and Sons, 2009.

Gruber, N., and Sarmiento, J. L.: Global patterns of marine nitrogen fixation and denitrification. Global Biogeochem. Cy., 11(2), 235-266, https://doi.org/10.1029/97GB00077, 1997.

Gruber, N., and Sarmiento, J. L.: Ocean biogeochemical dynamics: Princeton University Press, 2006.

Karl, D. M., Letelier, R., Hebel, D., Tupas, L., Dore, J., Christian, J., and Winn, C.: Ecosystem changes in the North Pacific subtropical gyre attributed to the 1991–92 El Niño. Nature, 373, 230, https://doi.org/10.1038/373230a0, 1995.

Lehmann, M. F., Sigman, D. M., McCorkle, D. C., Brunelle, B. G., Hoffmann, S., Kienast, M., Cane, G., and Clement, J.: Origin of the deep Bering Sea nitrate deficit: Constraints from the nitrogen and oxygen isotopic composition of water column nitrate and benthic nitrate fluxes. Global Biogeochem. Cy., 19(4), https://doi.org/10.1029/2005GB002508, 2005.

Mantyla, A. W., and Reid, J. L.: On the origins of deep and bottom waters of the Indian Ocean. J. Geophys. Res.-Oceans, 100(C2), 2417-2439, https://doi.org/10.1029/94JC02564, 1995.

Mariotti, A., Germon, J., Hubert, P., Kaiser, P., Letolle, R., Tardieux, A., and Tardieux, P.: Experimental determination of nitrogen kinetic isotope fractionation: some principles; illustration for the denitrification and nitrification processes. Plant soil, 62(3), 413-430, https://doi.org/10.1007/BF02374138, 1981.

McCartney, M. S.: Subantarctic Mode Water, A Voyage of Discovery, George Deacon 70th Anniversary Volume M. Angel, 103–119: Pergamon, New York, 1977.

McCartney, M. S.: The subtropical recirculation of mode waters. J. Mar. Res, 40(436), 427-464, 1982.

McClain, C. R., Signorini, S. R., and Christian, J. R.: Subtropical gyre variability observed by ocean-color satellites. Deep-Sea Res. Pt. II, 51(1), 281-301, https://doi.org/10.1016/j.dsr2.2003.08.002, 2004.

Michaels, A., Olson, D., Sarmiento, J., Ammerman, J., Fanning, K., Jahnke, R., Knap, A., Lipschultz, F., and Prospero, J.: Inputs, losses and transformations of nitrogen and phosphorus in the pelagic North Atlantic Ocean. Biogeochemistry, 35(1), 181-226, https://doi.org/10.1007/BF02179827, 1996.

Minagawa, M., and Wada, E.: Nitrogen isotope ratios of red tide organisms in the East China Sea: A characterization of biological nitrogen fixation. Mar. Chem., 19(3), 245-259, https://doi.org/10.1016/0304-4203(86)90026-5, 1986.

Monteiro, F. M., and Follows, M.: Nitrogen fixation and preferential remineralization of phosphorus in the North Atlantic: Model insights. Eos, Transactions, American Geophysical Union, 87(36), 2006.

Montoya, J. P., Carpenter, E. J., and Capone, D. G.: Nitrogen fixation and nitrogen isotope abundances in zooplankton of the oligotrophic North Atlantic. Limnol. Oceanogr., 47(6), 1617-1628, https://doi.org/10.4319/lo.2002.47.6.1617, 2002.

Montoya, J. P., and McCarthy, J. J.: Isotopic fractionation during nitrate uptake by phytoplankton grown in continuous culture. J. Plankton Res., 17(3), 439-464, https://doi.org/10.1093/plankt/17.3.439, 1995.

Muromtsev, A.: Osnovnye cherty gidrologii Indiiskogo okeana (The Main Features of Indian Ocean Hydrology). Gidrometeoizdat, Leningrad, 1959.

Murphy, J., and Riley, J. P.: A modified single solution method for the determination of phosphate in natural waters. Anal. Chim. acta, 27, 31-36, https://doi.org/10.1016/S0003-2670(00)88444-5, 1962.

Paulsen, H., Ilyina, T., Six, K. D., and Stemmler, I.: Incorporating a prognostic representation of marine nitrogen fixers into the global ocean biogeochemical model HAMOCC. J. Adv. Model. Earth Sy., 9(1), 438-464, https://doi.org/10.1002/2016MS000737, 2017.

Pickard, G., and Emery, W.: Descriptive physical Oceanography, 249 pp. Pcrgamon, Tanytown, NY, 1982.

Piola, A. R., and Gordon, A. L.: Intermediate waters in the southwest South Atlantic. Deep-Sea Res., 36(1), 1-16, https://doi.org/10.1016/0198-0149(89)90015-0, 1989.

Quadfasel, D. R., and Schott, F.: Water-mass distributions at intermediate layers off the Somali Coast during the onset of the southwest monsoon, 1979. J. Phys. Oceanogr., 12(12), 1358-1372, https://doi.org/10.1175/1520-0485(1982)012<1358:WMDAIL>2.0.CO;2, 1982.

Rafter, P. A., DiFiore, P. J., and Sigman, D. M.: Coupled nitrate nitrogen and oxygen isotopes and organic matter remineralization in the Southern and Pacific Oceans. J. Geophys. Res.-Oceans, 118(10), 4781-4794, https://doi.org/10.1002/jgrc.20316, 2013.

Redfield, A. C.: On the proportions of organic derivatives in sea water and their relation to the composition of plankton. James Johnstone memorial volume, 176-192, 1934.

Redfield, A. C.: The influence of organisms on the composition of seawater. The sea, 2, 26-77, 1963.

Reid, J. L.: On the total geostrophic circulation of the South Pacific Ocean: Flow patterns, tracers and transports. Prog. Oceanogr., 16(1), 1-61, https://doi.org/10.1016/S0079-6611(97)00012-8, 1986.

Reid, J. L.: On the total geostrophic circulation of the South Atlantic Ocean: Flow patterns, tracers, and transports. Prog. Oceanogr., 23(3), 149-244, https://doi.org/10.1016/0079-6611(89)90001-3, 1989.

Rixen, T., and Ittekkot, V.: Nitrogen deficits in the Arabian Sea, implications from a three component mixing analysis. Deep-Sea Res. Pt. II, 52(14-15), 1879-1891, https://doi.org/10.1016/j.dsr2.2005.06.007, 2005.

Schott, F. A., and McCreary, J. P.: The monsoon circulation of the Indian Ocean. Prog. Oceanogr., 51(1), 1-123, https://doi.org/10.1016/S0079-6611(01)00083-0, 2001.

Sharma, G.: Transequatorial movement of water masses in the Indian Ocean. J. Mar. Res., 1976.

Sigman, D. M., Altabet, M. A., McCorkle, D. C., Francois, R., and Fischer, G.: The δ15N of nitrate in the southern ocean: Consumption of nitrate in surface waters. Global Biogeochem. Cy., 13(4), 1149-1166, https://doi.org/10.1029/1999GB900038, 1999.

Sigman, D. M., Altabet, M. A., McCorkle, D. C., Francois, R., and Fischer, G.: The δ15N of nitrate in the Southern Ocean: Nitrogen cycling and circulation in the ocean interior. J. Geophys. Res.-Oceans, 105(C8), 19599-19614, https://doi.org/10.1029/2000JC000265, 2000.

Sigman, D. M., and Casciotti, K. L.: Nitrogen isotopes in the Ocean. In J. H. Steele, K. K. Turekian and S. A. Thorpe (Eds.), Encyclopedia of ocean sciences (pp. 1884-1894). New York: Elsevier, 2001.

Sigman, D. M., Robinson, R., Knapp, A., Van Geen, A., McCorkle, D., Brandes, J., and Thunell, R.: Distinguishing between water column and sedimentary denitrification in the Santa Barbara Basin using the stable isotopes of nitrate. Geochem. Geophy. Geosy., 4(5), https://doi.org/10.1029/2002GC000384, 2003.

Sigman, D. M., Granger, J., DiFiore, P. J., Lehmann, M. M., Ho, R., Cane, G., and van Geen, A.: Coupled nitrogen and oxygen isotope measurements of nitrate along the eastern North Pacific margin. Global Biogeochem. Cy., 19(4), https://doi.org/10.1029/2005GB002458, 2005.

Sigman, D. M., Karsh, K. L., and Casciotti, K. L.: Ocean process tracers: nitrogen isotopes in the ocean, Elsevier Ltd, 2009.

Sverdrup, H. U., Johnson, M. W., and Fleming, R. H.: The Oceans: Their Physics, Chemistry, and General Biology. Prenlice Hall NY, 1942.

Talley, L. D.: Antarctic intermediate water in the South Atlantic The South Atlantic (pp. 219-238): Springer, https://doi.org/10.1029/95JC00858, 1996.

Talley, L. D.: Closure of the Global Overturning Circulation Through the Indian, Pacific, and Southern Oceans, Schematics and Transports. Oceanography, 26(1), 80-97, 2013.

Toole, J. M., and Warren, B. A.: A hydrographic section across the subtropical South Indian Ocean. Deep-Sea Res. Pt. I, 40(10), 1973-2019, https://doi.org/10.1016/0967-0637(93)90042-2, 1993.

Wada, E., and Hattori, A.: Natural abundance of 15N in particulate organic matter in the North Pacific Ocean. Geochim. Cosmochim. Ac., 40(2), 249-251, https://doi.org/10.1016/0016-7037(76)90183-6, 1976.

Ward, B., Devol, A., Rich, J., Chang, B., Bulow, S., Naik, H., et al.: Denitrification as the dominant nitrogen loss process in the Arabian Sea. Nature, 461(7260), 78, 2009.

Warren, B. A.: Transindian hydrographic section at Lat. 18 S: Property distributions and circulation in the South Indian Ocean. Deep-Sea Res., 28(8), 759-788, https://doi.org/10.1016/S0198-0149(81)80001-5, 1981.

Waser, N., Harrison, P., Nielsen, B., Calvert, S., and Turpin, D.: Nitrogen isotope fractionation during the uptake and assimilation of nitrate, nitrite, ammonium, and urea by a marine diatom. Limnol. Oceanogr., 43(2), 215-224, https://doi.org/10.4319/lo.1998.43.2.0215, 1998.

Williams, R. G., and Follows, M. J.: The Ekman transfer of nutrients and maintenance of new production over the North Atlantic. Deep-Sea Res. Pt. I, 45(2-3), 461-489, https://doi.org/10.1016/S0967-0637(97)00094-0, 1998.

Williams, R. G., and Follows, M. J.: Physical transport of nutrients and the maintenance of biological production Ocean biogeochemistry (pp. 19-51): Springer, 2003.

Woodberry, K. E., Luther, M. E., and O'Brien, J. J.: The wind-driven seasonal circulation in the southern tropical Indian Ocean. J. Geophys. Res.-Oceans, 94(C12), 17985-18002, https://doi.org/10.1029/JC094iC12p17985, 1989.

Wurl, O.: Practical guidelines for the analysis of seawater: CRC press, 2009.

Wüst, G.: Die Stratosphäre. Wissenschaftliche Ergebnisse der Deutschen Atlantischen Expedition auf dem Vermessungs- und Forschungsschiff "Meteor" 1925-1927. 6(1,2), Jg., S. 109-288, 1935.

Wyrtki, K.: The oxygen minima in relation to ocean circulation. Paper presented at the Deep Sea Research and Oceanographic Abstracts, https://doi.org/10.1016/0011-7471(62)90243-7, 1962.

Wyrtki, K.: Oceanographic atlas of the international Indian Ocean expedition: National Science Foundation, 1971.

Wyrtki, K.: Physical oceanography of the Indian Ocean The biology of the Indian Ocean (pp. 18-36): Springer. https://doi.org/10.1007/978-3-642-65468-8_3, 1973.

You, Y.: Intermediate water circulation and ventilation of the Indian Ocean derived from water-mass contributions. J. Mar. Res., 56(5), 1029-1067. https://doi.org/10.1357/002224098765173455, 1998.

You, Y., and Tomczak, M.: Thermocline circulation and ventilation in the Indian Ocean derived from water mass analysis. Deep-Sea Res. Pt. I, 40(1), 13-56. https://doi.org/10.1016/0967-0637(93)90052-5, 1993.